Renewable Energy 235 (2024) 121386

Contents lists available at ScienceDirect

Renewable Energy

journal homepage: www.elsevier.com/locate/renene

Enhancing the hot water yield in low enthalpy geothermal systems in Sri Lanka

Dilshan Bandara [a,*], Jeroen Smit [a], Rodolfo O. Christiansen [a], Deepal Subasinghe [b], Stefan Wohnlich [a], Thomas Heinze [a]

[a] *Institute of Geology, Mineralogy and Geophysics, Ruhr-University Bochum, Universitätsstraße 150, 44801, Bochum, Germany*
[b] *National Institute of Fundamental Studies, Hanthana Road, Kandy, Sri Lanka*

ARTICLE INFO

Keywords:
Low-enthalpy geothermal systems
Near surface geophysics
Geothermal energy
Cost-efficient geothermal explorations
Sri Lanka

ABSTRACT

Global interest in low-enthalpy geothermal systems has emerged as a result of rising fossil fuel prices as well as a desire to reduce CO_2 emissions. However, in equatorial regions such as Sri Lanka, geothermal energy remains often unexploited, mainly because there is no need for space and district heating. The comparatively low temperatures and discharge rates of natural thermal springs are also insufficient for industrial or agricultural applications.

In Sri Lanka, hot water bearing faults are obscured by clay filled depressions of very low hydraulic conductivity. The clay limits the natural discharge rates of the hot water and leads to heat loss as well as mixing of thermal water with cold shallow groundwater. Identifying the near-surface hot-water bearing faults underneath the clay layer enables specifically targeted drilling operations. Bypassing the clay layer increases discharge rates and heat flow, hence enabling industrial and agricultural usage of the geothermal waters. Thus, comparably simple measures can put the geothermal resources of Sri Lanka to good use.

1. Introduction

The use of geothermal energy as a green energy source has received great attention in recent years [1]. Initially, geothermal systems associated with volcanic or active tectonics were favoured in most cases due to the typically elevated geothermal gradients in these environments, which facilitate heat exploitation. Exploration of low-enthalpy geothermal systems has intensified over the past decade due to increasing energy demands and technological advances that allow the use of heat and power from sources with temperatures below 100 °C [2]. As a result, geothermal systems in tectonically quiet (non-magnetic) cratons were also preferred for the investigation of geothermal exploitations [3]. Yet, natural discharge temperatures and flow rates of these systems are often too low for such kind of applications.

However, in equatorial countries such as Sri Lanka, where geothermal energy is not needed for district heating, the economic and ecological potential of geothermal energy resources often remains underexploited. The use of all 9 known natural hot springs in Sri Lanka is currently limited to recreational activities (Fig. 1). This is mainly due to the low outflow rates (5–10 l/min) and intermediate outflow temperatures (45 °C–72 °C) of the natural hot springs [4]. By chance, the 13m manmade artesian well at Padiyathalawa (PAD) was drilled into a hot water upwelling fault, which resulted in higher discharge rate (~150 l/min) and temperature (~55 °C) compared to the neighbouring naturally flowing hot springs. This evidences the presence of significant amounts of pressurized hot water at shallow depths and highlights the importance of proper identification of the hot-water bearing faults to boost future geothermal development in natural low-enthalpy systems.

All known hot springs in Sri Lanka are located on the margins of clay-filled depressions (Figs. 1 and 2) [6]. Remote sensing results show that regional-scale faults cross these clay-filled zones with multiple secondary faults, which are more likely to be hot water-bearing near-surface faults/fractures (Fig. 2). But in the field, the clay obscures the exact locations of these potentially hot water-bearing secondary faults.

The circulation of hot water in faults can affect the physical properties of the contacted zones in various ways: the alteration of subsurface electrical conductivities as a result of high mineralization and higher temperatures [7,8], and the existence of additional electric currents in the subsurface caused by the hot water upwelling zones [9,10]. Geophysical methods can be used to identify these changes in the

* Corresponding author.
E-mail address: dilshan.bandara@rub.de (D. Bandara).

https://doi.org/10.1016/j.renene.2024.121386
Received 26 February 2023; Received in revised form 16 February 2024; Accepted 15 September 2024
Available online 16 September 2024

physical properties of subsurface rocks. For example, the electrical resistivity and self-potential methods can then be used to identify hot water flow paths in more detail [9,10]. Therefore, with the aim of identifying these faults, we followed a geophysical approach that included electrical resistivity and self-potential surveys.

Based on the following criteria, we selected two study sites in Sri Lanka, Padiyathalawa (PAD) and Mahapelessa (MAH): The 13-m shallow drilled well in PAD indicates high flow rates of hot water in shallow fractures, implying that a detailed study of the terrain may lead to the discovery of additional hot water resources. The low discharge (~5–10 l/min) and relatively low-temperature (~45 °C) MAH hot spring was selected due to its accessibility and potential for significant future impact on the tourism industry as the geothermal potential of the area is developed.

The aim the of this paper is to identify near-surface hot water bearing fault(s) by a simple, cost-efficient method to enable adoption and usage by local communities and authorities. Based on our conceptual model (Fig. 3), drilling directly into the fault will result in higher outflow temperatures and flow rates, similar to the well drilled at Padiyathalawa. The thermal water rises near to the surface from an over pressurized system at depth through water bearing faults. The bedrock is covered by a paddy clay filled depression inhibiting further water flow towards the surface. The fluid path with highest hydraulic conductivity to the surface, and the path with the highest-pressure gradient, is along the boundary of weathered bedrock and the paddy clay. Hence, hot springs are primarily found at the borders of the paddy clay fields. Due to the pressurized state of the uprising thermal water, it will partially infiltrate in to the aquifer system in the weathered bedrock, mix with shallow groundwater and potentially form low-temperature water springs in some distance to the paddy clay field based on topography and water levels. Hence, bypassing the clay layer by drilling will provide a substantial enhancement to the useable geothermal energy in Sri Lanka.

2. Geological setting

Sri Lanka is an island in the Indian Ocean, south of India and close to the equator (Fig. 1a). High-grade Precambrian metamorphic rocks form the basement of the island, except for the northwest and the coastal plains [11,5]. The upper 10–20 m of the subsurface is typically weathered under the influence of the tropical climate. River valleys and local depressions are partially filled with alluvial and/or lake sediments.

Sri Lanka has 9 naturally occurring hot springs [12]. Peak circulating temperatures calculated using silica and Na-Li geothermometers range from 97 °C to 120 °C [4]. Outflow temperatures range from 45 °C to 72 °C between hot springs. The discharge rates of all naturally occurring hot springs range from 5 to 10 L/min. The electrical conductivity of the PAD hot springs is 1210 μS/cm while in the MAH is 7360 μS/cm due to a high mineralization of the thermal waters [4]. The natural groundwater has electrical conductivity value of 593 μS/cm in the PAD and in the MAH it is 7290 μS/cm [4]. Premasiri et al. [13] and Chandrajith et al. [4] proposed that hot water circulates through a fault network and then rises to the surface through the same or a different fault zone. The small

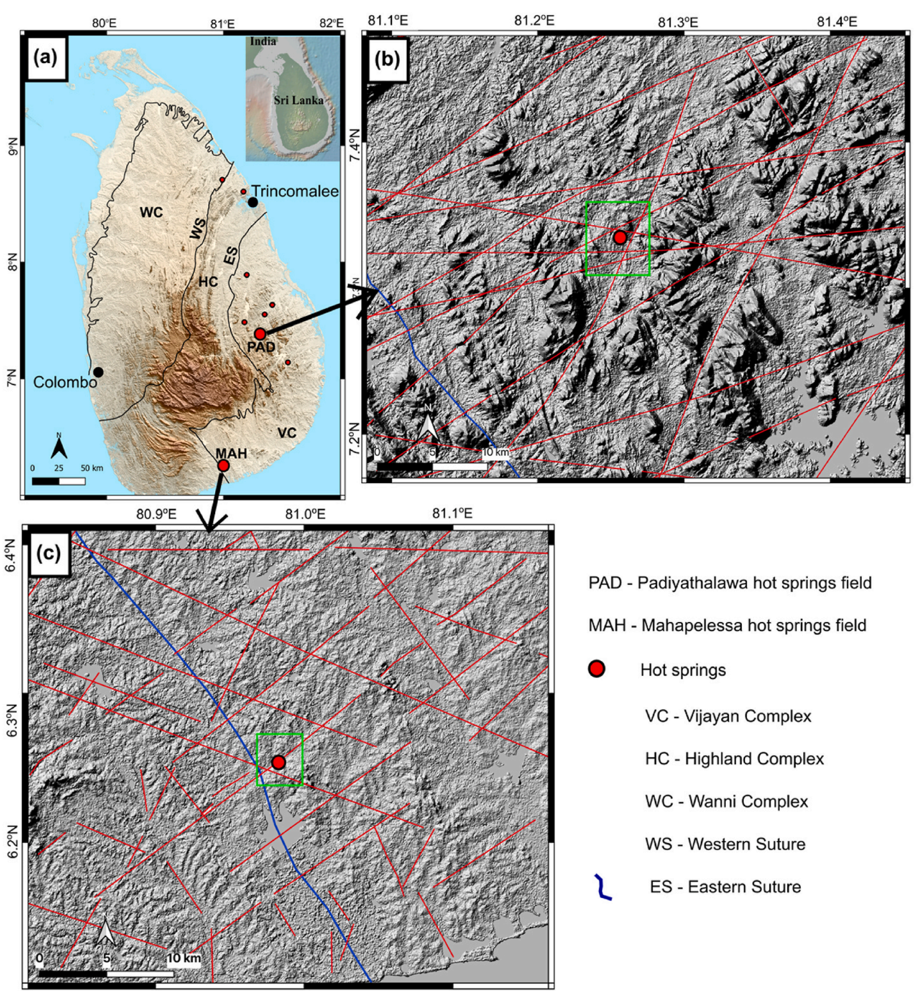

Fig. 1. Locations of the known hot water spring fields in Sri Lanka. (a). The location of hot springs is marked on the shaded relief map. Large red dots two study sites, PAD and MAH (Modified after [5]). (b) & (c) Locations of hot springs on the shaded relief map and regional scale fault/fracture network of two sites. The map area of Fig. 4 is demarcated with dashed green colour box.

contrast in electric conductivity between thermal spring water and ambient groundwater at MAH indicates a very strong influence of the thermal spring water on the groundwater system with little dilution. The more substantial contrast at PAD indicates only little or none mixing of thermal spring and groundwater [14].

The present-day fault network in Sri Lanka is the result of successive tectonic activities since the opening of the Indian Ocean 160 Ma ago [15,16]. The most recent and still active faults result from the NNW-SSE compression in the Indian Ocean and the collision between the Eurasian and Indian plates [15,17]. Larger faults have widths of 10–30 m, while fault zones can be up to 600 m wide and can be traced for over 100 km distance [16].

The 10–12 m overburden in the PAD hot spring field consists mainly of weathered metamorphic rocks and paddy clay. The area around the hot springs is surrounded by paddy fields and minor forest cover [6]. A small ~10 m wide stream flows through the hot spring area in an NNW direction. The surrounding area of the MAH hot spring field is entirely used as a paddy field, and the hot spring is also located in paddy clay. The direction of the small stream that crosses the area has been changed by local farmers to suit their land use [18].

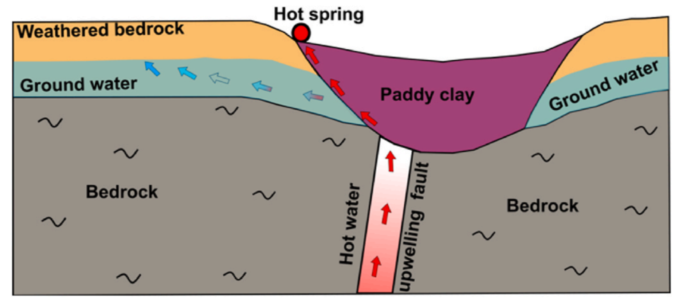

Fig. 3. Conceptual model of near-surface hot water upwelling through the overburden to the hot springs. Red arrows show the hot water flow in the overburden after upwelling from the fault in the bedrock. Note the importance of the clay/weathered bedrock interface as flow paths for hot water in the overburden since hot springs in both (PAD and MAH) hot water springs are located at clay/weathered bedrock margins. Note that the springs are located along the fault zone.

3. Methods

3.1. Remote sensing

We used digital elevation models and shaded relief maps generated from 30 m resolution SRTM-1 arc second global digital elevation satellite imagery (https://earthexplorer.usgs.gov) to identify the prominent structures (e.g. faults, fractures) in PAD (6 × 5 km^2) and MAH (6 × 5 km^2) (Fig. 4). Faults and fractures were mapped according to the elevational ruptures identified in the shaded relief map and the DEM. Later, satellite images and georeferenced published geological maps were used to avoid misinterpretation of shear zones, lithological boundaries and man-made structures from identified faults and fractures. Shaded relief mapping, georeferencing and fault analysis were carried out in QGIS. Field work was carried out later to ground truth the identified structures.

3.2. Geophysical surveys

3.2.1. Two-dimensional electrical resistivity tomography (2D ERT) survey

The 2D ERT surveys were conducted using an AGI Ministing R1 resistivity meter with a 28-electrode system. Two profiles were conducted for each of the hot spring fields. The orientations and locations of the ERT profiles were chosen to be in close proximity to the hot water spring (s) and to cross the estimated faults or fractures at a high angle.

The Wenner-Schlumberger array was used in both hot spring fields due to its sensitivity to horizontal and vertical structures, as well as its high signal strength in comparison to other arrays [19]. Electrode spacing along each survey profile was chosen to be between 4 and 7 m, based on geology and accessibility. The two PAD resistivity profiles are 189 m and 162 m, the two MAH profiles are 135 m and 108 m long. Data processing and inversion were performed using the open source Python-based program RESIPY 3.3 [20]. Prior to the inversion, noisy data points (data spikes in the pseudo sections) and negative apparent resistivity data points were removed. The inversion process used finite element forward modelling and least squares constrained smoothness methods. Several iterations of inversions were performed until the root mean square (RMS) values of the calculated and predicted percentage differences were less than 3 %. Temperature correction is generally applied to electrical resistivity tomograms, especially in high-enthalpy geothermal exploration [21]. However, based on the equation in Hermans et al. [22], the calculated resistivity changes due to the temperature contrast of 20–30 °C between the hot water and mean ambient air temperature at the two sites (45 °C in MAH and 55 °C in PAD) is around 20–30 Ωm and therefore small compared to the overall resistivity

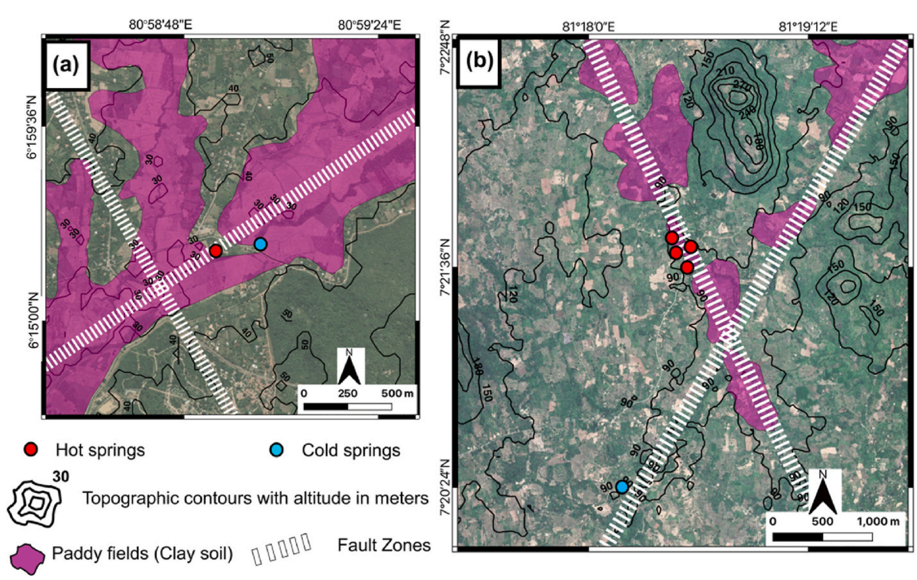

Fig. 2. Locations of hot spring(s) in relation to the paddy (clay) soil in the topographic maps of two sites, (a). MAH, (b). PAD.

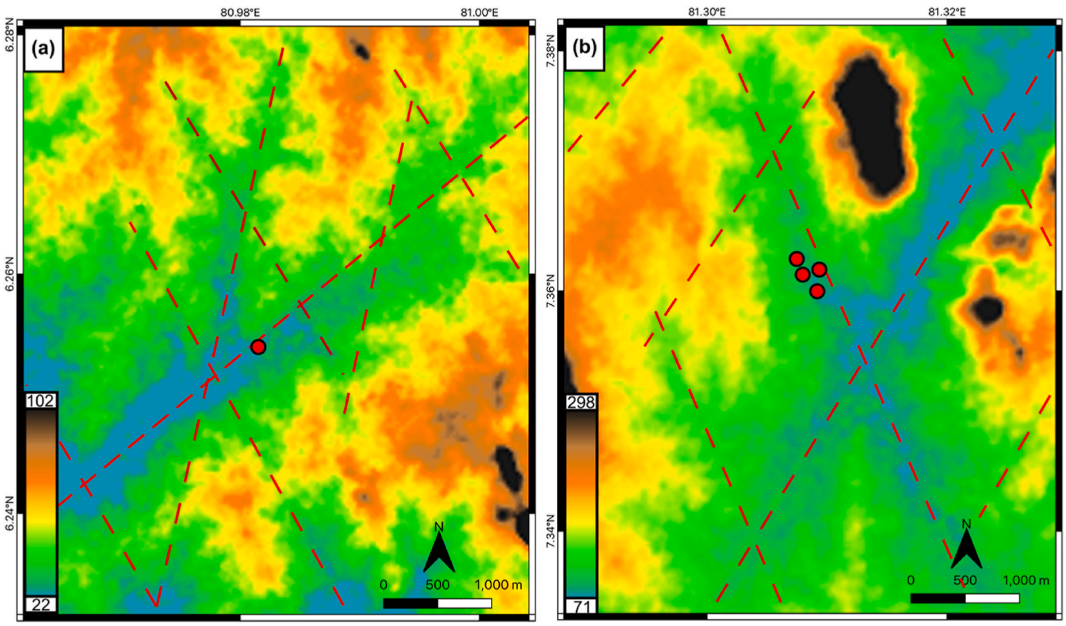

Fig. 4. Fault/fracture network in the two study sites, (a). MAH (b) PAD. Altitudes values are marked in meters w.r.t mean sea level.

contrast in the tomograms. Therefore, no temperature corrections are applied for the ERT results of the present study (cf [23]).

3.2.2. *Self potential method*

At both sites, self-potential (SP) data were collected along two ERT profiles whenever possible [10,24]. However, due to accessibility and ground conditions, minor changes had to be made to the SP data collection points from the ERT profiles (Fig. 5). The SP data were acquired using two non-polarized Cu/CuSO4 electrodes with rubber sealed top and wooden bottom in combination with high impedance voltmeters with a sensitivity of 0.1 mV. The fixed base method was used in the acquisition of the SP data at both sites because of its ability to detect smaller SP anomalies as compared to the gradient method [25]. The base (reference) electrode location was chosen to be centred within the SP surveyed area. To measure the residual potential between the two electrodes, measurements were taken at the smallest electrode separation. The measured residual voltage static shift between two electrodes was then corrected in data processing. Therefore, all data represent the potential difference between the measured and reference points. We made the SP measurements over a short period of time (less than an hour) so that the telluric current effect and other meteorological effects that could affect the SP measurements in a tropical environment such as the present two study sites have negligible influences. We performed repeated measurements on all data points to minimise measurement error. The uncertainty of the SP measurements was determined as 0.2 mV from repeated measurements.

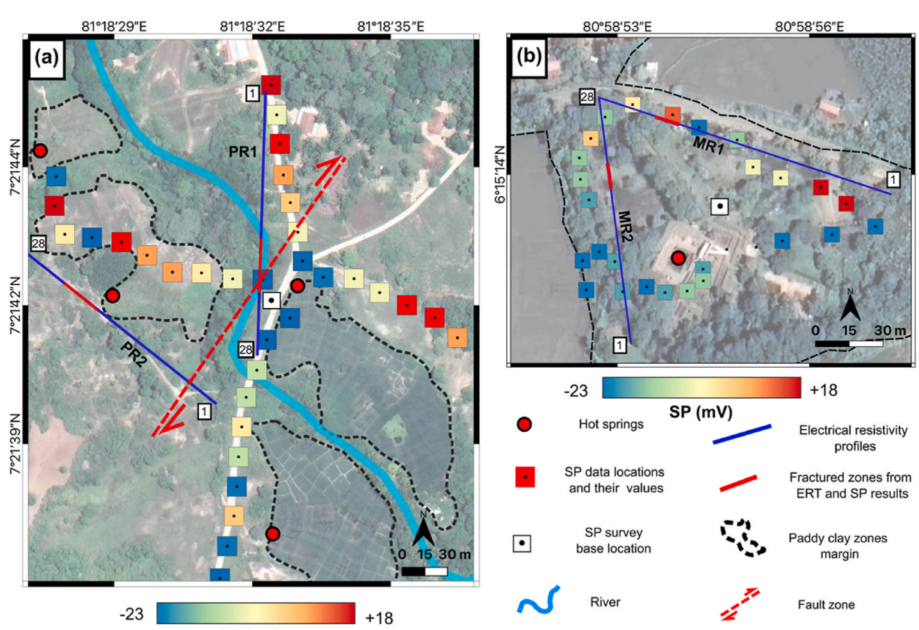

Fig. 5. ERT survey profiles and SP data points in the study areas. (a). PAD hot spring field. (b). MAH hot spring field.

4. Results

4.1. Fault/fracture network

Fault/fracture analysis results for the MAH and PAD hot spring fields are shown in Fig. 4. Highly fractured zones are identified for both hot spring fields. Three main fault/fracture orientations are identified in the MAH spring fields as NE-SW, NNE-SSW and NW-SE (Fig. 4a). Two prominent fault/fracture orientations in the PAD spring field are NE-SW and NW-SE (Fig. 4b). Hot water springs are located along faults/fracture while the springs locations are closely located to faults/fracture intersection zones in both hot spring fields.

4.2. Electrical resistivity and self-potential surveys

Electrical resistivity profiles and self-potential data point locations for the PAD and MAH sites are shown in Fig. 5.

Both PR1 and PR2 resistivity profiles at PAD show low electrical resistivity (<100 Ωm) for the upper 10 m (Fig. 6a and b), below which resistivity increases to over 400 Ωm. Two near vertical low resistivity zones (PF1) and (PF2) (Fig. 6) are seen in both profiles. The self-potential anomalies along the two resistivity profiles vary from −20 mV to +17 mV and from −15 mV to +3 mV, respectively (Fig. 6a). Two sharp negative SP anomalies coincide with the two near vertical low resistivity zones (PF1 and PF2) in the resistivity profiles (Fig. 6a and b).

The two resistivity tomograms (MR1 and MR2) in the MAH hot spring field show low resistivity values (<50 Ωm) in the upper 10–15 m and higher resistivity values at depth (>200 Ωm) (Fig. 6c and d). Two near-vertical zones of low resistivity are identified in both profiles and are designated MF1 and MF2 (Fig. 6c and d). Self-potential anomalies along the MR1 and MR2 profiles vary from −14 to +15 mV and −7 to +21 mV, respectively. The locations of the two positive SP anomalies match with zones of low resistivity (MF1 and MF2) (Fig. 6c and d). In the MR2 profile, the positive self-potential anomaly is slightly shifted to the north with respect to the near-vertical MF2 low resistivity zone (Fig. 6d).

5. Discussion

5.1. Faults/fractures and hot water springs

In both the MAH and PAD fields, hot springs are located along fault zones and also in close proximity to fault/fracture intersection zones (Figs. 1 and 4). This indicates that the increased permeability in the fault/fracture zones and their intersections facilitates the rise of deep hot water to the surface. Similar settings have been reported in several other hot water springs, as in the Tet Fault hot spring system in France, where most hot springs are located near the intersection of subsidiary faults with the Tet Fault [26], in the Yunnan-Tibet geothermal belt [27], in the Great Basin in the USA and in western Turkey [28]. The presumably higher permeability at fault/fracture zones and their intersections shortens the ascending time, decreasing temperature loss, subsequently forming a hot water spring at the surface.

Based on our fault/fracture network analysis, undiscovered hot springs and shallow hot water-bearing faults are most likely to be found at fault/fracture zones and their intersections in two of the study areas, as well as in the other hot water spring fields in the country. This structural information is therefore vital in narrowing down potential sites for future geothermal exploration.

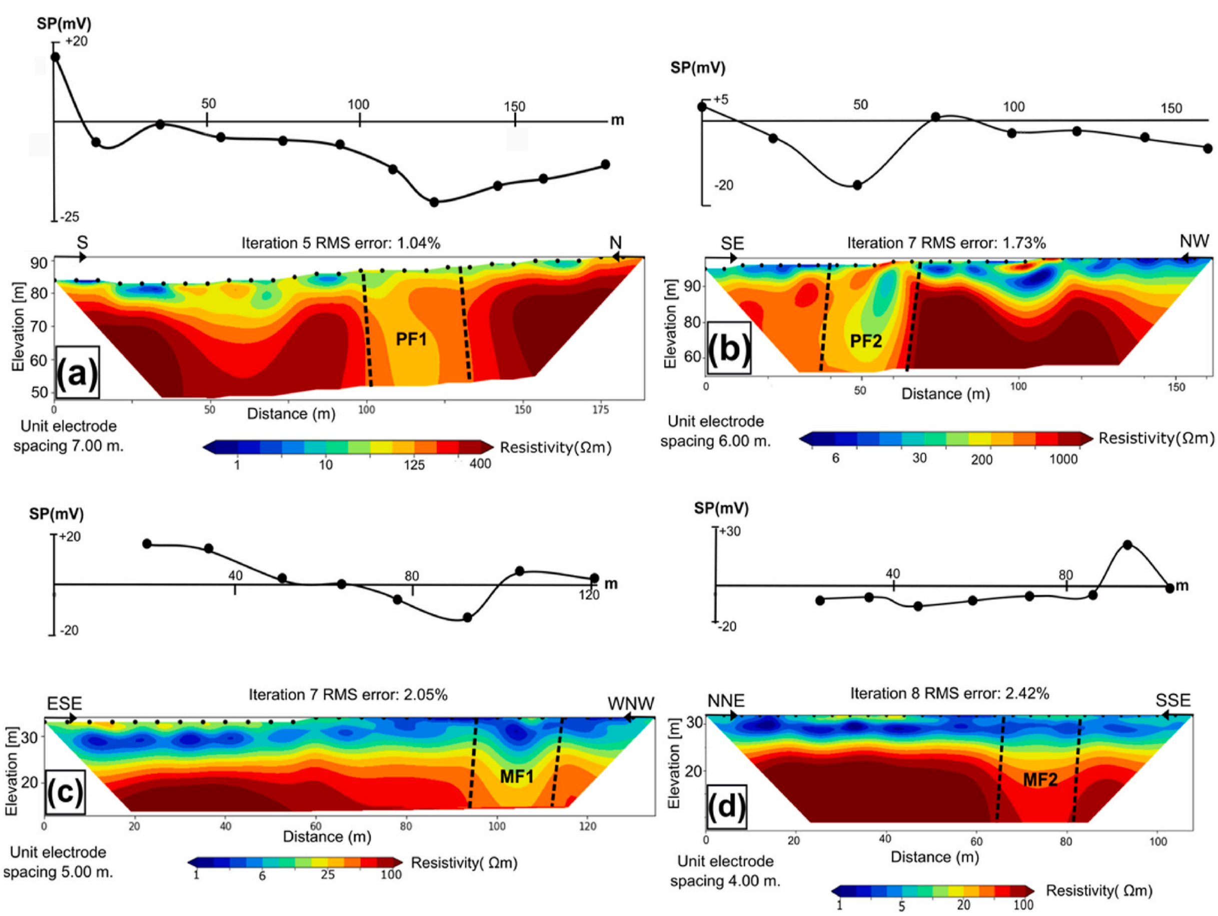

Fig. 6. Inverted ERT results with SP anomaly along the resistivity survey profile of both PAD and MAH hot spring fields. (a) Profile PR1; (b) Profile PR2; (c) Profile MR1; (d) Profile MR2. The uncertainty of SP measurements is 0.02 mV, therefore they cannot be visualised in the SP anomaly graphs.

In the case of a shallow hot water-bearing fault/fracture, drilling into a hot water-bearing fault zone further reduces upwelling times while increasing flow rates by eliminating the interaction of hot water with potentially low-hydraulic conductivity near-surface structures and shallow water bodies. However, detailed geophysical surveys will need to be carried out in such potential zones to confirm the existence of shallow hot water bearing fault/fracture zones.

5.2. Electrical resistivity and S-P interpretations

The electrical resistivity and self-potential results help to further constrain the location of upwelling geothermal water, especially near the surface. In the PAD hot spring field, both the PR1 and PR2 ERT profiles show approximately 30 m wide, near vertical zones of low resistivity (Fig. 6a and b). These two zones (PF1 and PF2) appear to represent two highly fractured and therefore highly permeable zones in the NNW-SSE fault zone through which highly mineralized hot water of low electric resistivity is upwelling. The shallow layer of low electric resistivity with a varying thickness of around 10m corresponds with the clay layer found in the field.

Consistent with the results of the resistivity survey, both the SP anomaly profiles along PR1 and PR2 show a clear negative SP anomaly directly above the low resistivity zones of PF1 and PF2. This could be due to changes in the self-potential of nearby zones as a result of the hot water upwelling [10]. Therefore, we interpret these two zones as weak zones (sub-faults/fractures) within the main NNW-SSE fault zone in the PAD hot spring field through which the hot water upwells.

Similar negative SP anomalies have been observed at two other locations, one to the south and one to the northwest of the PAD area, approximately 100 m from the two main weak zones identified above (Fig. 5a). As there are also two hot springs in close proximity to these two zones, we propose that these two zones are also possible hot water upwelling zones, although electrical resistivity results would be required to confirm this interpretation.

In the MAH hot spring field, ERT profiles show two low resistivity zones approximately 15 m wide (MF1 and MF2). The SP anomaly profiles show two positive SP anomalies in line with these two low resistivity zones. The slight shift of the positive SP signal away from the weak zone identified by the ERT profile in MR2 is likely because the SP profile was not orthogonal to the fault orientation (Fig. 6d). Therefore, using the same argument as for the SP and ERT interpretations in PAD, we interpret MF1 and MF2 as two weak zones where highly-mineralized hot water upwells causing the resistivity anomaly. In addition to that, probable weak zone MF1 and MF2 are aligned with the direction of the NE – SW faults zone identified from the DEM and magnetic anomaly maps. This suggests that MF1 and MF2 are weak zones through which the deeply circulating hot water in the NE-SW fault zone up well to the surface. The generally lower electric conductivity at MAH compared to PAD might respond to the generally increased electric conductivity of the groundwater at MAH.

5.3. Potential applications of geothermal energy in Sri Lanka

At present, hot water springs in Sri Lanka are only used for recreational activities, especially as a tool for tourist attractions. The low discharge rates of the natural hot water springs are not sufficient for other use cases. However, the drilled artesian hot water well in PAD provides a decent amount of thermal energy which can be used for advanced applications. Any future usage of the geothermal energy in Sri Lanka needs to increase discharge and temperature. The only possibility for this is to identify more drilling targets, such as the location of the PAD artesian well. The methodology and results presented in this paper can be used to identify potential drilling locations in the shallow subsurface that promise significantly increased flow rates and elevated temperatures. The current study also identified two probable zones of hot water fields. This also provides a promising indication that more hot water can be extracted for future geothermal energy applications.

Utilizing geothermal energy for the above mentioned agricultural and industrial applications will provide much needed economic development and stability to the rural areas surrounding the hot springs in Sri Lanka. As exploration expands into areas not yet known for geothermal manifestations, drilling opportunities may also arise in more densely populated areas. This will further enhance the application of geothermal energy.

As seen in every hot spring field in Sri Lanka, a relatively shallow 10–15 m clay layer limits the flow rate and causes a significant drop in temperature. This is due to the low fluid permeability of the clay, which increases the upwelling time of hot water in the clay. In general, clay soils do not contain a water table. Therefore, although the clay has a negative impact on the hot water flow rate and discharge temperature, it prevents the rising hot water from mixing with the terrain's cold groundwater flow. Conversely, weathered bedrock that contains groundwater will mask the rising hot water by mixing the hot water with the cold groundwater. This can explain why all known natural hot springs in Sri Lanka are located in clay or clay-weathered bedrock interface.

By bypassing this clay layer, nearly half of the peak circulating temperature can be achieved at surface outflow. Due to the overpressurized state of the system, the wells are artesian and no pumping is required, further benefitting the energy balance of the geothermal systems. As the drilled artesian hot water well show no signs of clogging by mineral precipitation after 40 years of production [4,14], it can be expected that maintenance costs will also be low for drill hole and casing.

Currently, the natural hot water springs provide an extractable thermal power $\dot{E}\,(W)$ of 13–16 kW assuming an annual mean groundwater temperature of 27 °C [29] as cooling agent with

$$\dot{E} = \dot{m} \bullet C_p \bullet \Delta T,$$

using mass flow $\dot{m}\,(kg/(m^3 \bullet s))$, and temperature difference $\Delta T\,(^\circ C)$ as provided in Table 1, and specific heat capacity $C_p = 4\,200\,J/(kg \bullet {}^\circ C)$. The drilled 13 m deep artesian well provides 300 kW, which is about 15 times that of a natural hot spring.

In the present study, we identified one additional locations of possible hot water upwelling similar to the location of the artesian well in the PAD hot spring field. Assuming that this zone also delivers the same outflow temperatures and flow rates, the thermal energy that can be extracted at PAD is around 600 kW. A negative interaction between multiple drilling wells and the natural springs needs to be examined, as well as the potential for additional drilling locations further away from the hot springs. Potentially, drilling close to the hot springs might cause the natural springs to fall dry.

Conversion of geothermal heat to electrical energy typically requires at least 60 °C of temperature difference for operation when using Organic Rankine Cycles (ORC). The warmest natural hot spring in Kapurella has an outflow temperature of about 72 °C and therefore is the most promising location for power generation. However, its economic viability could be challenged by more cost-effective renewable energy sources for direct electric power generation, such as solar power, in despite of the baseload capability of the geothermal energy.

Generally, in low enthalpy geothermal systems the direct use of the heat is energetically beneficial to avoid further loss of energy during the conversion into electric energy.

In Sri Lanka, most areas around hot spring fields are rural and semi-arid. In the context of Sri Lanka, suitable direct heat applications include agricultural drying, fish drying, shrimp farming, sugar processing, paper mills operations, and recreational facilities such as hot water pools, saunas and steam baths.

Table 1
Possibly heat energy extraction for the two study sites.

Hot spring field	Outflow temperature (°C) [a]	Groundwater temperature of the terrain (°C) [b]	Hot water Outflow rate (l/min)	Calculated heat Energy (kW)*
MAH- Natural	45	27	10	12.6
PAD- Natural	50	27	10	16.1
PAD- Artesian	55	27	150	294

C = specific heat capacity of water (4.186 J/g°C).
[a] [4].
[b] [12].

6. Conclusions

Here we present a comparably simple methodology based on remote sensing and geophysics to identify hot-water bearing faults close to the surface. This method will boost geothermal related applications in Sri Lanka without the need of significant financial investments. Drilling into the identified probable hot water bearing lineaments will most likely result in significantly increased flow rates and elevated temperatures as the obstructive clay layer on top of the fault is bypassed.

The present methodology will enable the industrial usage of the geothermal resources of Sri Lanka and provide a much-needed economic boost to the respective rural areas around all hot springs in Sri Lanka. Relying on locally available technology and instruments, the proposed workflow provides a timely, simple, and cost-efficient method to substantially increase the extractable geothermal heat in low-enthalpy systems in Sri Lanka and elsewhere.

Data availability

Geophysical survey data are available upon request to the Corresponding author at dilshan.bandara@rub.de. All other data and software used in the article are cited and listed in the reference list.

CRediT authorship contribution statement

Dilshan Bandara: Conceptualization, Investigation, Methodology, Visualization, Writing – original draft, Writing – review & editing. **Jeroen Smit:** Conceptualization, Investigation, Supervision, Visualization, Writing – review & editing. **Rodolfo O. Christiansen:** Formal analysis, Investigation, Methodology, Writing – review & editing. **Deepal Subasinghe:** Resources, Supervision, Writing – review & editing. **Stefan Wohnlich:** Funding acquisition, Supervision, Writing – review & editing. **Thomas Heinze:** Conceptualization, Investigation, Methodology, Supervision, Writing – review & editing.

Declaration of competing interest

The authors declare that they have no known competing financial interests or personal relationships that could have appeared to influence the work reported in this paper.

Acknowledgments

D.B. acknowledges the German Academic Exchange Service (DAAD) for funding the doctoral project. National Science Foundation of Sri Lanka Grant RG/2016/EQ/11 is acknowledged for providing geophysical equipment.

References

[1] L. Rybach, Geothermal power growth 1995-2013-a comparison with other renewables, Energies 7 (2014) 4802–4812, https://doi.org/10.3390/en7084802.
[2] D. Chandrasekharam, J. Bundschuh, Low-enthalpy Geothermal Resources for Power Generation, CRC Press, 2008, pp. 1–151, https://doi.org/10.1080/00207233.2010.498602.
[3] I.S. Moeck, Catalog of geothermal play types based on geologic controls, Renew. Sustain. Energy Rev. 37 (2014) 867–882, https://doi.org/10.1016/j.rser.2014.05.032.
[4] R. Chandrajith, J.A.C. Barth, N.D. Subasinghe, D. Merten, C.B. Dissanayake, Geochemical and isotope characterization of geothermal spring waters in Sri Lanka: evidence for steeper than expected geothermal gradients, J. Hydrol. 476 (2013) 360–369, https://doi.org/10.1016/j.jhydrol.2012.11.004.
[5] P.G. Cooray, The Precambrian of Sri Lanka: a Historical Review: Precambrian Research, vol. 66, 1994, pp. 3–18, https://doi.org/10.1016/0301-9268(94)90041-8.
[6] D. Bandara, J. Smit, T. Gunatilake, S. Riechelmann, S. Wohnlich, T. Heinze, Fluid upwelling and alluvial controls on spring localization: an example from Sri Lanka, Groundwater for Sustainable Development 26 (2024) 101289, https://doi.org/10.1016/j.gsd.2024.101289.
[7] S.K. Garg, J.W. Pritchett, P.E. Wannamaker, J. Combs, Characterization of Geothermal Reservoirs with Electrical Surveys: Beowawe Geothermal Field: Geothermics, vol. 36, 2007, pp. 487–517, https://doi.org/10.1016/j.geothermics.2007.07.005.
[8] A. Mandal, A.K. Basantaray, A. Chandroth, U. Mishra, Integrated geophysical investigation to map shallow surface alteration/fracture zones of Atri and Tarabalo hot springs, Odisha, India: Geothermics 77 (2019) 24–33, https://doi.org/10.1016/j.geothermics.2018.08.007.
[9] R.F. Corwin, D.B. Hoover, The self-potential method in geothermal exploration, Geophysics 44 (1979) 226–245, https://doi.org/10.1190/1.1440964.
[10] K. Richards, A. Revil, A. Jardani, F. Henderson, M. Batzle, A. Haas, Pattern of shallow ground water flow at Mount Princeton Hot Springs, Colorado, using geoelectrical methods, J. Volcanol. Geoth. Res. 198 (2010) 217–232, https://doi.org/10.1016/j.jvolgeores.2010.09.001.
[11] A. Kröner, P.G. Cooray, P.W. Vitanage, Lithotectonic subdivision of the precambrian basement in Sri Lanka: the crystalline crust of Sri Lanka, summary of research of the German-Sri Lankan consortium, Geol. Surv. Dept. (1991) 1–5. Sri Lanka.
[12] K.S.G.S. Priyadarshanee, Z. Pang, E.A.N.V. Edirisinghe, H. A. Dharmagunawardhane, H.M.T.G.A. Pitawala, J.D.C. Gunasekara, I.A.N.D. P. Tilakarathna, Deep groundwater recharge mechanism in the sedimentary and crystalline terrains of Sri Lanka: a study based on environmental isotopic and chemical signatures of spring water, Appl. Geochem. (2021) 105174, https://doi.org/10.1016/j.apgeochem.2021.105174.
[13] H.M.R. Premasiri, D.S. Wijeyesekera, S. Weerawarnakula, U.G.A. Puswewala, Formation of Hot Water Springs in Sri Lanka: Engineer, vol. 39, Journal of the Institution of Engineers, Sri Lanka, 2006, p. 7, https://doi.org/10.4038/engineer.v39i4.7195.
[14] D.T. Jayawardana, D.T. Udagedara, A.A.M.P. Silva, H.M.T.G.A. Pitawala, W.K. P. Jayathilaka, A.M.N.M. Adikaram, Mixing geochemistry of cold water around non-volcanic thermal springs in high-grade metamorphic terrain, Sri Lanka For.: Chem. Erde 76 (2016) 555–565, https://doi.org/10.1016/j.chemer.2016.10.003.
[15] K.V.W. Kehelpannala, Deformation of a high-grade Gondwana fragment, Sri Lanka For.: Gondwana Res. 1 (1997) 47–68, https://doi.org/10.1016/s1342-937x(05)70005-8.
[16] K.V.W. Kehelpannala, H. Wada, L. Ranaweera, N. Hamana, Cataclastic Rocks from the Granulite Terrain of Sri Lanka: Evidence for Younger Brittle Deformation of the Exhumed Lower Crust, Geoscience Reports of the Shizuoka University, 2006, pp. 9–19.
[17] S. Cloetingh, R. Wortel, Stress in the indo-Australian plate, Tectonophysics 132 (1986) 49–67, https://doi.org/10.1016/0040-1951(86)90024-7.
[18] B. Mapa, in: A.E. Hartemink (Ed.), The Soils of Sri Lanka, Springer Netherlands, 2020, pp. 1–119, https://doi.org/10.1007/978-3-030-44144-9_1.
[19] H. Al-Amoush, J. Rajab, E. Al-Tarazi, A.R. Alshabeeb, R. Al-Adamat, A. Al_Fugara, Electrical resistivity tomography modeling of vertical lithological contact using different electrode configurations: Jordan, Journal of Earth and Environmental Sciences 8 (2017) 27–34.
[20] G. Blanchy, S. Saneiyan, J. Boyd, P. McLachlan, A. Binley, ResIPy, an intuitive open source software for complex geoelectrical inversion/modeling, Comput. Geosci. 137 (2020) 104423, https://doi.org/10.1016/j.cageo.2020.104423.
[21] L. Lévy, et al., Electrical resistivity tomography and time-domain induced polarization field investigations of geothermal areas at Krafla, Iceland: comparison to borehole and laboratory frequency-domain electrical observations, Geophys. J. Int. 218 (2019) 1469–1489, https://doi.org/10.1093/gji/ggz240.
[22] T. Hermans, F. Nguyen, T. Robert, A. Revil, Geophysical methods for monitoring temperature changes in shallow low enthalpy geothermal systems, Energies 7 (2014) 5083–5118, https://doi.org/10.3390/en7085083.

[23] A. Carrier, F. Fischanger, J. Gance, G. Cocchiararo, G. Morelli, M. Lupi, Deep electrical resistivity tomography for the prospection of low- to medium-enthalpy geothermal resources, Geophys. J. Int. 219 (2019) 2056–2072, https://doi.org/10.1093/gji/ggz411.
[24] X. Bolós, G. Cifuentes, J.L. Macías, G. Sosa-Ceballos, F. Garcia-Tenorio, M. Albor, Geophysical imaging of fluid circulation and its relation with the structural system of Cerritos Colorados geothermal field, La Primavera caldera (Mexico), J. Volcanol. Geoth. Res. 369 (2019) 238–249, https://doi.org/10.1016/j.jvolgeores.2018.11.015.
[25] S. Barde-Cabusson, A. Finizola, N. Grobbe, A practical approach for self-potential data acquisition, processing, and visualization, Interpretation 9 (2021) T123–T143, https://doi.org/10.1190/INT-2020-0012.1.
[26] A. Taillefer, R. Soliva, L. Guillou-Frottier, E. Le Goff, G. Martin, M. Seranne, Fault-related controls on upward hydrothermal flow: an integrated geological study of the têt fault system, Eastern Pyrénées (France), Geofluids, v. 2017 (2017), https://doi.org/10.1155/2017/8190109.
[27] Y. Wu, X. Zhou, L. Zhuo, G. Tao, J. Ma, Y. Wang, Structural controls of the northern Red River Fault Zone on the intensity of hydrothermal activity and distribution of hot springs in the Yunnan-Tibet geothermal belt, Geothermics 109 (2023) 102641, https://doi.org/10.1016/j.geothermics.2022.102641.
[28] J. Faulds, M. Coolbaugh, V. Bouchot, I. Moeck, K. Oğuz, O. Cedex, Characterizing Structural Controls of Geothermal Reservoirs in the Great Basin , USA , and Western Turkey : Developing Successful Exploration Strategies in Extended Terranes, C, World, 2010, pp. 25–29. https://hal-brgm.archives-ouvertes.fr/hal-00495884/document.
[29] R. Rubasinghe, S.K. Gunatilake, R. Chandrajith, Geochemical characteristics of groundwater in different climatic zones of Sri Lanka, Environ. Earth Sci. 74 (2015) 3067–3076, https://doi.org/10.1007/s12665-015-4339-1.